Desert RHex Technical Report: Jornada and White Sands Trip

Sonia Roberts[1], Jeff Duperret[1], Aaron M. Johnson[1], Scott van Pelt[2], Ted Zobeck[2], Nick Lancaster[3], and Daniel E. Koditschek[1]

[1]Electrical and Systems Engineering, University of Pennsylvania
[2]USDA Agricultural Research Service
[3]University of Nevada Desert Research Institute

November 2014

Abstract

Researchers in a variety of fields, including aeolian science, biology, and environmental science, have already made use of stationary and mobile remote sensing equipment to increase their variety of data collection opportunities. However, due to mobility challenges, remote sensing opportunities relevant to desert environments and in particular dune fields have been limited to stationary equipment. We describe here an investigative trip to two well-studied experimental deserts in New Mexico with D-RHex, a mobile remote sensing platform oriented towards desert research. D-RHex is the latest iteration of the RHex family of robots, which are six-legged, biologically inspired, small (10kg) platforms with good mobility in a variety of rough terrains, including on inclines and over obstacles of higher than robot hip height.

Contents

List of Figures

List of Tables

1 Introduction

1.1 Stationary and mobile remote sensor networks

Autonomous remote sensing platforms can collect data for surveys that would otherwise be unobtainable, either because the experimental environment is too dangerous (e.g. volcanoes [1], typhoons [2]) or too distant (e.g. extraterrestrial rovers on Mars [3, 4]), or simply because the volume of data needed for the survey would require too long a time period of infrequent sampling to be practical for a human researcher (e.g. the autonomous sensor network pioneered in [5]; see [6] for context and a discussion).

The longest history of remote sensor networks has been in oceanographic research, with both stationary [7] and mobile remote sensors [8, 9]. Single semi-autonomous vehicles have been used in remote sensing applications since the 1950s with the invention of the Special Purpose Underwater Research Vehicle, the first autonomous underwater vehicle, which was developed for research purposes in the University of Washington's Applied Physics Lab to study submarine turbulence [10, 11]. Since then, underwater research vehicles have found application in underwater structure monitoring and exploration [12] (see [9] for a review), the study of naturally occurring turbulence and turbulent mixing [13, 14], oceanographic monitoring [15, 16, 17] (see [18] for a discussion), environmental and weather monitoring [19, 20, 21, 22, 23], commercial applications such as oil rig or deep ocean telecommunication cable monitoring [24], and biological studies (e.g., [7]; see [13] for a general discussion). The field is sufficiently well-developed now that research focus has moved to coordination of fleets of autonomous vehicles [25, 26] by surface vehicles [27, 28, 29, 30] capable of autonomous navigation and cooperative localization [31], with remotely operated vehicles existing now as a platform to develop new sensors and other technologies on these lower-risk platforms [32].

The life and earth sciences would benefit from this same exploration of the utility of remote sensing platforms for research on land. While the majority of research in these fields has historically been performed with stationary sensor nodes, scientists have begun integrating mobile robots into networks with stationary sensor nodes [33, 6, 34, 35]. Stationary ecological surveys have been well-received [36] in the earth and life sciences, and there is growing interest in mobile sensor applications [19] and even some research [21].

1.2 Sensors for aeolian research

Research into aeolian processes involving entrainment, transport and deposition of sand ($> 63\mu$m diameter particles) and dust ($< 63\mu$m) has a long history of field experiments using fixed-position sensors. Studies can be conveniently divided into long-term "monitoring" studies in which key variables are measured routinely, and "event-based" studies in which intensive measurements of processes are carried out during periods of particle movement.

Commonly used sensors measure wind speed and direction, turbulence inten-

sity, dust concentration, and sand and dust flux at fixed locations. Deployment of such instrumentation is time- and personnel-intensive, and requires constant maintenance. Especially in areas of complex terrain (e.g. coastal dune systems), siting of the instruments is critical to obtaining meaningful datasets [37].

Mobile instrumentation packages have the potential to dramatically increase the ability to measure spatial and temporal patterns of aeolian processes at an event scale. One example is the PISWERL (Portable InSitu Wind Erosion Laboratory) [38]. This instrument package can be used to measure soil erodibility and dust emissions potential at multiple sites as a result of its small size and easy portability, largely replacing large, expensive, and cumbersome inline field wind tunnels as a means to assess the spatial variability of dust emissions. PISWERL provides multiple measurement datasets, such that statistical analyses can be used to determine patterns of dust emission potential.

1.3 Remote sensing of aeolian processes

The majority of remote sensing studies of aeolian processes have involved orbital (satellite) and airborne sensors. Although most use of remote sensing data has involved studies of landforms (see [39] for a review), orbital data sets have provided valuable data on the location and dynamics of dust sources [40, 41]; sand composition and transport pathways [42]; sand availability (moisture content) [43] and dune movement and rates of sand flux [44].

Ground-based remote sensing studies have used Ground Penetrating Radar (GPR) to probe dune sedimentary structures [45]; terrestrial laser scanning to determine surface roughness of dust sources [46]; patterns of erosion and deposition and sand moisture content on dunes and beaches [47].

1.4 Mobile remote sensing in desert environments

Previous research on mobile sensors in desert environments has largely focused on extraterrestrial exploration [4, 48, 49, 50] and while many locomotory and perceptual problems are shared between navigation on Martian and Earth deserts, we intend to study saltation of fine particles and interactions of wind with vegetation, which are not perceptual problems that exist on Mars. Though technology exists for all the necessary sensory capabilities, there are not "robot-ready" commercially available versions of all relevant sensors.

Furthermore, current locomotor capabilities for robots oriented towards data collection in sandy environments are insufficient for our needs. Whereas previous robust, legged [49, 50] and wheeled rover [51] systems have been built to collect data slowly over a long period of time for extraterrestrial missions, moving a robot only short distances (much less than 1km), we will need to capture data during relatively short, 20-minute aeolian events from multiple locations within 5km, necessitating a much faster robot that is unlikely to get stuck in topsoil [52] and is free from a tether [49].

1.5 Applications to search and rescue

Not only will the ground be of variable compliance, but it may be unsteady or unreliable [53]. There may be hostile environmental factors to be avoided such as heat from still-burning fires, natural gas leakages or live wires, or sharp metal [53], increasing the importance of being able to handle more benign obstacles (e.g., large boulders; mud) so as to increase the number of possible routes for a robot that minimize contact with hostile obstacles. Not only are floors likely to be canted, but the ground is likely to change inclination quickly [54]. Dust may also be present [55], or if the disaster is accompanied by flooding, water [54]. There may or may not be large, recognizable objects [55] that could be used for navigation and registration. Indeed, disaster settings present an almost unlimited variety of possible types of terrains. The ability to move quickly through an unreliable, sandy, inclined environment is therefore of immediate interest to search and rescue operations.

1.6 The Jornada research desert

The Jornada Experimental Range is managed by the USDA, Agricultural Research Service Range Management Research Unit established to produce new knowledge of ecosystem processes for development of technologies for remediation and management of desert rangelands. Their programs comprised of long term scientific investigations, experiments that contribute to national research objectives, development of technologies applicable to land management, and synthesis of information for public use[1]. The Jornada conducts world-class research as demonstrated by designations as a USDA Long Term Agriculatural Research site (LTAR), a NSF Long-Term Ecological Research site (LTER), and a NSF National Ecological Observatory Network (NEON) participant. All programs include important projects investigating regional, national, and global issues. In addition, the Jornada is the home of the USDA Southwest Climate Hub.

The Jornada Experimental Range occupies an area 783km^2 located 40 km north of Las Cruces, NM. It is on the Jornada del Muerto Plain in the northern Chihuahuan Desert [56]. The landscape of the Jornada is typical of desert basins of the Basin and Range physiographic province and the Chihuahuan Desert. The region has abundant sunlight, low air humidity and wide ranges in daily temperature.

Aeolian processes and wind erosion have been studied for many years at the Jornada. In the 1930s, the change in the soil levels relative to benchmark stakes after measurement in 1980 revealed gross wind erosion rates of over 100 Mt yr^{-1} at some sites [57]. Measurements of sand flux in various plant communities at the Jornada demonstrated that values of mean, height-integrated, horizontal flux for mesquite-dominated sites were higher than those for other kinds of vegetation [58]. In a study of the effects vegetation on aeolian processes, many stationary wind sensors were used to measure shear stress in mesquite-dominated sites

[1] http://jornada.nmsu.edu/programs

[59]. A very recent study also used stationary measurements of wind speed to investigate the wind speed and sediment transport recovery in the lee of a vegetated and denuded nebka (coppice dune) within a dune field at the Jornada [60].

1.7 The White Sands national monument

The White Sands dunefield is the largest known gypsum dunefield in the world and covers an area of 500 km^2. It is located in the topographically-closed Tularosa Basin of the Rio Grande Rift in southern New Mexico. The dunefield is comprised of a central area of crescentic dunes up to 15m high, flanked on its north, east, and south sides by partially vegetated parabolic dunes. To the west is an extensive deflation plain (Alkali Flat), which constitutes the main source of sediment for the dunefield. A series of playas in which gypsum is precipitated occupy the lowest part of the basin and form the source of contemporaneous sediment supply to the dunefield. The dominant winds in the basin are from the SW and W during winter, with N-NW winds in the fall and winter and S-SSE in summer.

White Sands dunefield has established itself as a prominent natural laboratory for investigations of dune dynamics and sediments. As a result, the main features of the pattern of dune morphology, dune and interdune sediments, and recent geologic history are well documented [61, 62, 63, 64]. Dune dynamics and their impact on sedimentary processes are discussed by [65, 66, 67]. Recent work has focused on downwind changes in dune morphology in relation to changes in boundary layer winds as they cross the dunefield [68, 69]; as well as evolution of sediment characteristics [70]. The accessible and well-defined vegetation-free crescentic dune areas at White Sands are therefore an ideal location in which to test legged robots as a vehicle for remote sensing of aeolian processes.

2 Robot platform enabling mobility

The RHex robots [71] are biologically inspired, six-legged robots that are small enough for a human to carry in a backpack (10kg) but have a large, flat back (57 x 39cm) on which a variety of sensors can be mounted. The robot has been tested in a variety of environments, including flat desert terrain [71], obstacle fields with obstacles higher than robot hip height [72], and inclines in the form of hills and stairs [73].

Extensive locomotion research has been performed in RHex-like robots ranging in size from 1m to 10cm [74, 75, 76, 77, 78], and some effort has been made to increase performance in dry, granular media through gait modifications [78] and morphology adjustments [74]. There are two successful locomotory paradigms for these legged robots in sand: Rotary walking, a low-frequency locomotion paradigm in which legs intrude into the fluidized media until the penetration force is sufficient to solidify the granular media under the robot's foot and allow it to push off in preparation for the next stride; and swimming, a high-frequency

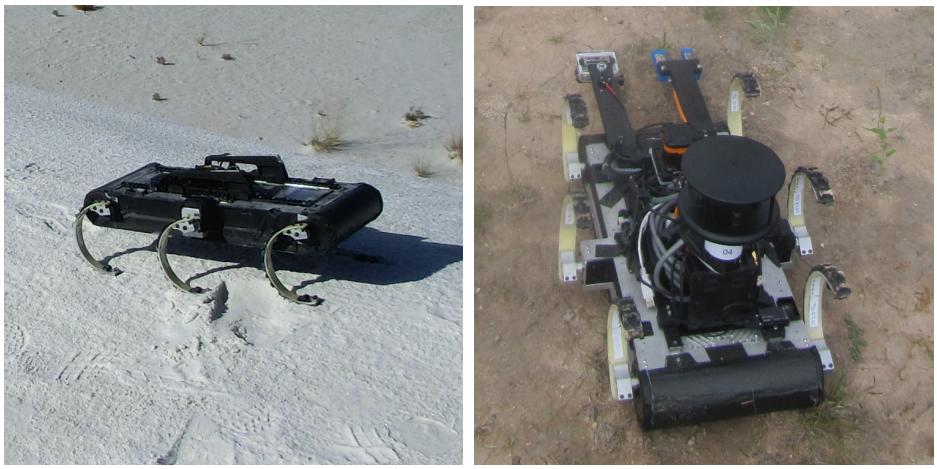

(a) The robot with no sensor payload

(b) The robot with Wenglor fork sensor, downward-facing camera, Hokuyo laser scanner, and Windsonic anemometer

Figure 1: D-RHex, with and without full sensor payload from this trip.

locomotion paradigm in which legs push through fluidized material that does not solidify [74, 76, 78].

Several other robot platforms that locomote well in sand have been developed, but none offer the same opportunity that the RHex family of robots does to carry a heavy load of sensors on a large, wide, flat back. A robot inspired by a lizard [79, 80] that fluidizes material around its body to swim beneath the surface of dry sand has also been studied [81] and this research contributed greatly to the generation of a new resistive force theory "terradynamics" for the behavior of objects intruding in dry granular media [82]. Hatchling sea turtles [83] inspired a robot capable of locomotion by rotated insertion of flippers [84]. More recently, modular robots using a snake-like sidewinding gait have been shown to locomote successfully up sandy slopes [85]. Finally, a clam-like robot also uses fluidization and solidification properties of granular media to bury and anchor itself quickly [86].

3 Sensor suite

D-RHex 2.0 (Desert Robot Hexapod 2.0; hereafter D-RHex) will be a new RHex-family robot, representing the desert-ready member of the X-RHex generation [87]; D-RHex 1.0 was a desert-optimized version of the early RHex robots with light shell coloration and a fan to push sand out. D-RHex differentiates itself from XRL, the X-RHex generation robot optimized for unladen agility [88, 89], and the base X-RHex model [71], by its specialization for sandy, hot environments, with light coloration, protective sealing tape, and wider legs with dimen-

sions determined by new research in dry granular media locomotion [90].

3.1 Field sensors adapted for robot use

3.1.1 Anemometer

An anemometer is an instrument used to measure wind speed, while a wind vane measures wind direction. For our mobile usage on D-RHex we find it convenient to use a 2-D Gill Windsonic anemometer[2] which gives the compact equivalent functionality of an anemometer and a wind vane in a single compact package with no moving parts. The largest of the sensors used on D-RHex, the cylindrical sensor is 142mm in diameter, 160mm tall, and weighs 0.5kg. Figure 2 shows the sensor and how it is mounted to the robot. As mounted, all wind measurements are taken parallel to the horizontal plane of the robot and about 180mm above the center of the robot. Therefore, they do not account for any vertical motions of the air or if the robot has a pitch or roll angle. The sensor could be used to measure wind speed and direction in other locations; for example if the sensor were mounted on a boom or arm it could measure wind in a vertical plane close to the desert surface.

Like many of the sensors described below, anemometers are often used at a stationary base station. We hope that the mobility conferred by RHex will allow a greater spacial resolution of a sensor network than conferred by a series of base stations. A mobile sensory platform also presents advantages in dynamically changing environments such as sand dunes as the mobile platform can easily shift locations of measurements as the environment changes. While the anemometer was used in most outdoor experiments at Jornada and White Sands, there was very little wind and therefore the outdoor anemometer data is not of significant interest. In future work we hope to put the anemometer to use in windy conditions to measure wind velocity with fine spacial resolution across an object of interest such as a dune crest on which it would be cumbersome to put many stationary instruments. Dune crests are a particularly compelling area to measure because they are hypothesized to play a significant role in the saltation process yet there is almost no dune crest data in the scientific literature.

To measure how the robot itself might affect wind measurments close to the surface, the sensor was placed at various distances from the robot in front of a large fan.

The hypothesis was that there could be wind disturbances at a downwind distance of up to five times the robot's body height, and upwind up to three times the robot's body height. Table 2d shows the measured wind speed in the forward direction at various distances upwind of the robot's body. For these experiments the robot was in a standing posture in front of a large fan. The results indicate that there is no difference in the interference from the robot body over the range of distances measured, as all measurements are within one standard deviation of each other.

[2] http://gillinstruments.com/products/anemometer/windsonic.htm

(a) The WindSonic 2-axis ultrasonic anemometer.

(b) The WindSonic mounted on D-RHex

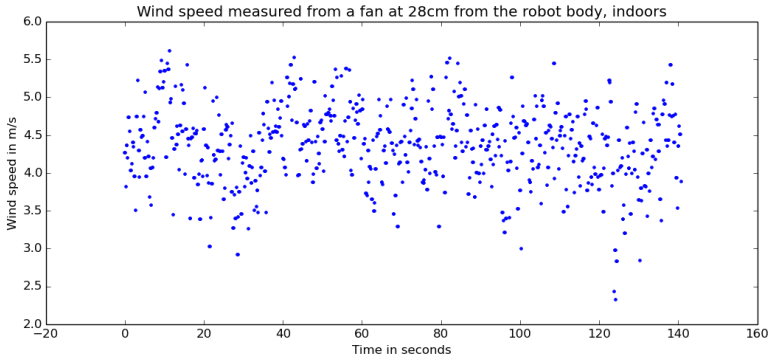

(c) Example data from the anemometer

Distance (cm)	Mean wind speed	Standard deviation
8	4.0697	0.5439
18	4.4862	0.5237
28	4.3671	0.5145
38	4.2920	0.5327
48	4.2602	0.6454

(d) Mean anemometer readings at a range of distances from the robot over two minutes of data collection.

Figure 2: The WindSonic anemometer

(a) D-RHex performing a pitching maneuver in front of a bush at White Sands.

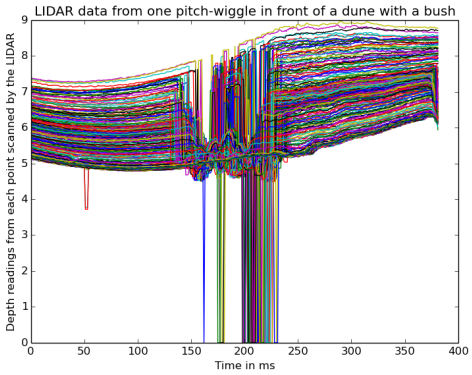

(b) The raw LIDAR data from the scan D-RHex is performing in (a). Each colored line represents datapoint collected over time from one angle relative to the robot. The smooth portion corresponds to the dune face, and the bush can be readily seen.

Figure 3: D-RHex was able to capture 3D point clouds of whole objects of interest by performing a pitching maneuver.

3.1.2 LIDAR

LIDAR is a remote sensing technique in which a laser beam is reflected off of a surface and measured back at the source. The distance of the object can then be estimated from time-of-flight while various other attributes about the object can be estimated by using amplitude or phase of the returned signal. Frequently the laser beam is actuated to rapidly achieve multiple measurements across a scene of interest and can be used to gather a 2- or 3-dimensional spacial point cloud.

In Jornada and White Sands a Hokuyo UTM-30LX LIDAR was used. This is a powerful and compact 2-D LIDAR designed for mobile applications and is significantly cheaper than comparable 3-D LIDAR models. It actively scans the azimuth and can be used to scan elevation if rotated 90 degrees when placed on the robot.

At White Sands, we experimented with obtaining 3D point clouds of obstacles of interest by pitching the robot slowly upwards while scanning the azimuth with th LIDAR scanner. This pitching maneuver was accomplished by laying the robot flat on the ground and then raising the body up using only the front two legs. In Figure 3 we present one example scan of data obtained using this maneuver.

In Jornada the desert surface was characterized by a primarily flat horizontal surface punctuated by large obstacles, typically low-lying mesquite trees or small dunes. In this scenario a horizontal 2-D LIDAR on a robot operating in the flat section is useful for detecting where these objects are in relation to the robot. In

(a) The Hokuyo UTM-30LX

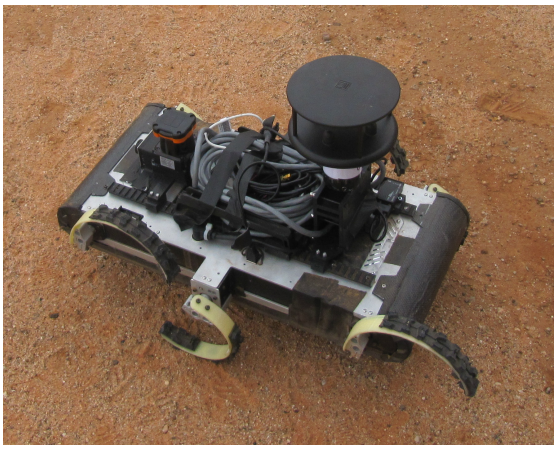

(b) The laser scanner mounted on D-RHex with WindSonic anemometer

Figure 4: The Hokuyo outdoor laser scanner

particular, we were interested in taking various sensor measurements at known distances from these objects, which can be accomplished by LIDAR.

In Jornada we experimented with obtaining 3-D data of obstacles of potential interest on long walks. In one Jornada experiment we gradually approached a bush and stopped at known distances away to take sensor readings. Similarly, in another Jornada experiment we navigated between a series of small dunes using LIDAR for both obstacle avoidance and to provide features for later SLAM implementation. Using LIDAR in a dune environment is complicated by the fact that large dunes are largely featureless manifolds to a horizontal LIDAR, and that the robot often has trouble seeing the dune if it is on a concave portion of it.

The dunes at White Sand have been extensively mapped by airborne LIDAR to yield a 3-D inch-resolution map of the dunes using a drone aircraft. This type of remote sensing will undoubtedly become more common in the future and allow for high-resolution, large-scale mapping of the desert environment. It is possible that we could use this data to localize in the desert along with GPS. Because the dunes shift this airborne LIDAR could be off by as much as several feet over the course of a year. Importantly, the local LIDAR scans could be used in conjunction with these infrequent flyover studies to investigate movement of particular dunes of interest with much greater time resolution.

3.1.3 Wenglor fork

Airborne particle movement was measured using a YH03PCT8 Wenglor fork sensor. The Wenglor is a commercially available, low-cost, laser particle detector that can be used to detect small particle movement in the air stream. The sensor

works by projecting a thin laser beam between an emitter and receiver, which is obscured to the receiver when a particle enters the beam. Isolated particles greater than 40 μm in diameter passing through the laser beam are detected and the number of particles can be integrated over time to estimate the rate of airborne particle movement. This capability permits the detection of particle movement threshold, intensity of wind erosion event based on particle counts, and duration of wind erosion events.

Laboratory and field performance of the Wenglor for aeolian research has been described by Hugenholtz and Barchyn [91]. The Wenglor is able to count particles passing through the laser beam but it cannot detect particle diameter, and thus particle momentum. In addition, some particles may not be detected if there are so many particles in the air that some are obsured as they pass through the laser. Care must be taken to ensure that the lens is not contaminated with fine particles during measurement. This is generally not an issue with very sandy soils. In soils with significant fine material, the lens will need to be cleaned regularly.

We plan to use this sensor to measure saltation rate on the crest of a dune. By taking multiple measurements across a dune crest we hope to better understand how saltation rate varies along the crest. As with wind speed, saltation rate is strongly affected by the presence of the robot; however because of the small size of the sensor we were able to construct a small boom to project the sensor in front of the robot. This also gives us the ability to measure at different heights by pitching the robot either up or down.

Due to the lack of wind during the trip, the Wenglor fork sensor was tested on the robot by releasing sand in front of a large fan outdoors. The test setup and resulting data are shown in Figure 6. The plot shows that using the Wenglor we are able to measure the rate of particulate flow in the wind with an acceptable resolution.

3.1.4 Pyranometer

Remotely sensed surface albedo obtained from the earth-orbiting MODerate resolution Imaging Spectroradiometer (MODIS) platform has been successfully used to characterize surface characteristics in the deserts of North Africa and the Arabian peninsula [92]. More recently, a related measure of shadowing and angular reflectance has been used at smaller spatial scales and shorter measurement distances to estimate surface roughness and aerodynamic roughness lengths [93].

Surface albedo is often measured using paired pyranometers oriented normal to the surface and at 180° from each other. In this configuration, the intensity of incoming solar radiation and of reflected solar radiation are independently measured and compared. Pyranometers utilize differential heating of black and white surfaces containing embedded temperature measuring devices and have long (15 – 20s) response times. In order to obtain a measurement of albedo with short (1s) response times, silicon photocells may be utilized. Common applications of these photocells include camera light meters and optical security

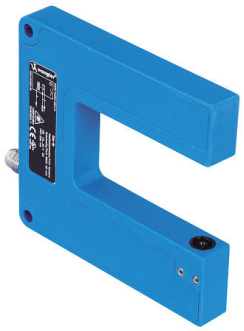

(a) The Wenglor sensor.

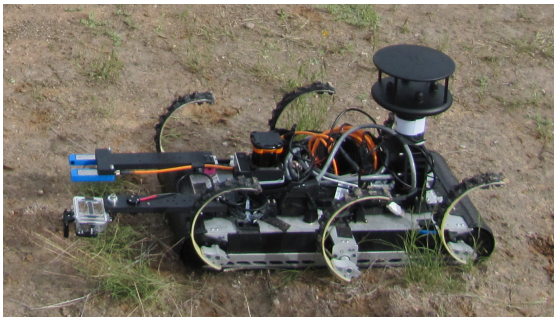

(b) The Wenglor mounted on D-RHex, along with anemometer, housing for downward-facing camera, and laser scanner.

(c) D-RHex on a dune crest at the White Sands national monument. Future experiments could involve taking measurements while traversing dune crests during wind events of interest.

Figure 5: The Wenglor fork sensor

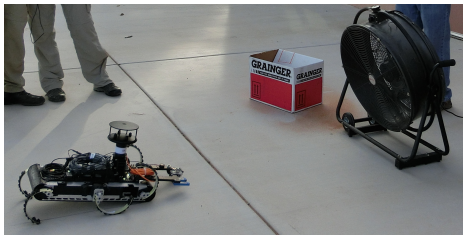

(a) The Wenglor fork sensor was tested by blowing sand towards the robot. By pitching the robot we are able to take measurements at a height of our choice; in this case the robot is pitched downwards to measure saltation rate immediately above the ground.

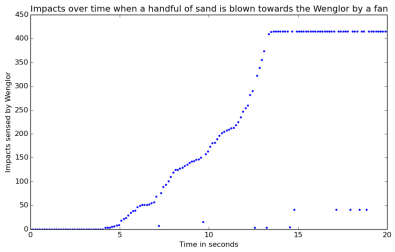

(b) The resulting data showing the rate of particles per second detected in the wind is shown to the right.

Figure 6: Wenglor sensor tests.

systems. Instruments with wireless data-streaming technology that can measure independently or integrate and produce a differential measure of multiple photocells are available on the market for less than $2,000.00. These instruments are small, lightweight, and would be easily adapted to deployment on a legged robot. Lightweight spectroradiometers are also available on the market and would allow more flexible real-time measurement of surface characteristics including vegetation and biotic crusts, but these instruments are nearly an order of magnitude more expensive than the paired photocells.

For this test run, we mounted a Li-Cor Pyranometer LI-200 on an arm 6cm from the robot's body and pointed it at the ground. Next to the pyranometer on the same arm was a downward-facing GoPro Hero3 camera mounted at 11cm from the robot body, so that pyranometer data could be correlated with pictures of the actual soil type and vegetation. See Figure 1b for a picture of the pyranometer mounted on the robot, behind the downward-pointing GoPro camera on the robot's left arm. Unfortunately, the pyranometer that we tested in this initial run did not have an appropriate sensitivity to light reflected from the ground at a distance of less than 20 cm, but we have demonstrated the ability to collect such data with our robot platform and should be able to collect more reliable data with a better-informed sensor choice in future experiments.

3.1.5 Downward-facing camera

Small digital cameras capable of continuous image capture and still image extraction are easily mounted on a legged robot and have been tested in this study. The images are satisfactory to allow post-processed image analysis, including simple analyses such as measuring the frequency of pixels containing a specified color and more sophisticated techniques such as image segmentation to discern

(a) D-RHex with downward facing camera on the left arm

(b) A sample image taken by the downward-facing GoPro camera

Figure 7: D-RHex with downward facing camera and sample image

spatial patterns and textures [94]. Spectral image analysis has evolved rapidly and has allowed development of algorithms to detect high-contrast patterns in the image and texture files and for user-defined boundaries to refine low-contrast boundaries in images [95]. Using these and other image analysis tools, it should be possible to accurately and efficiently characterize the surfaces traversed by our legged robots. Furthermore, with development time and improvements with real-time image processing speed, the down-facing camera may provide input to improve gait control over changing surfaces.

Screenshot	**Average green channel value**	**Average red channel value**
1	117.4258	116.0005
2	119.7212	124.1101
3	111.3310	110.0267
4	111.7091	111.6910
5	88.7316	94.2892
6	145.8261	146.2469
7	122.7805	122.0904
8	109.9676	111.4884
9	133.0944	137.8026
10	133.2262	138.7921

Table 1: Pixel values from green and red channels from the 10 screenshots in Figure 8 from the downward-facing camera.

For the time being, we have provided only a preliminary analysis of the average green and red channel values of pixels in a few sample screenshots of the ground; however, for future analysis it will be possible to classify images of the ground as coming from a variety of substrate types such as dead plant cover, live plant cover, particles over 2mm, loose soil, and crusted soil. In some

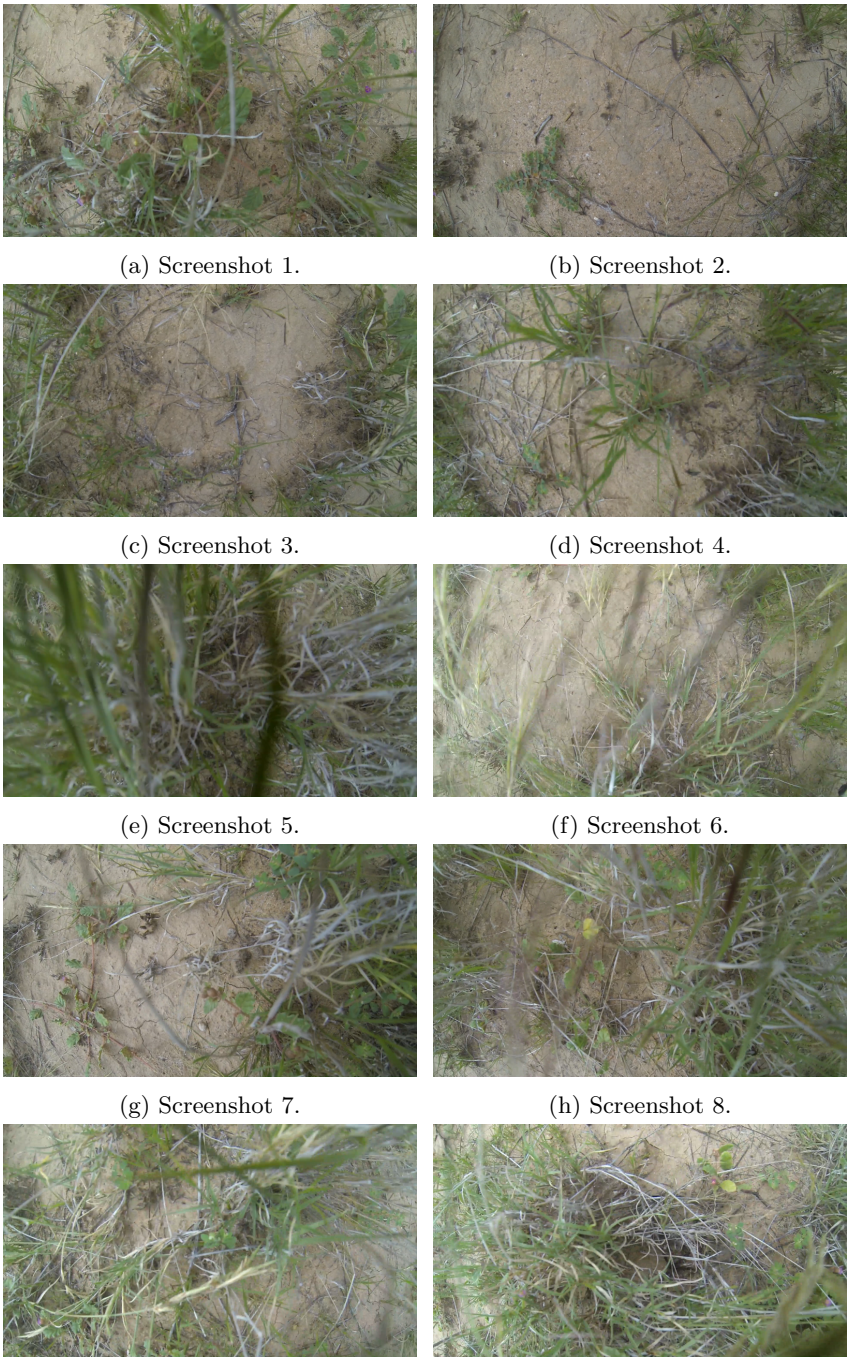

(a) Screenshot 1. (b) Screenshot 2.

(c) Screenshot 3. (d) Screenshot 4.

(e) Screenshot 5. (f) Screenshot 6.

(g) Screenshot 7. (h) Screenshot 8.

(i) Screenshot 9. (j) Screenshot 10.

Figure 8: The example screenshots used in the analysis in Table 1.

areas it may be possible to determine the type of crust present (physical or biologic). By recording continuously, we should also be able to observe more relevant metrics to earth science research, such as the amount of bare ground $>$ 30cm wide.

3.1.6 Forward-facing camera

The forward-facing camera could allow a remote user to control the direction of robot travel and to avoid major obstacles too large to safely cross. It also may be used in conjunction with the LIDAR to assess proximity to surface obstacles and vegetation and to assess the size, porosity, and flexibility of vegetation elements. These parameters control the effect the vegetation has on the aerodynamic roughness coefficient and thus on the wind speed profile over the vegetation community on a macro scale spatially and in the inter-vegetation spaces on a smaller spatial scale. The size and porosity of obstacles also affects aeolian transport by providing impact points for the entrained sediments and inter-canopy eddies which remove the energy from the wind. These factors control the spatial heterogeneity observed with wind speed profiles, surface wind impingement, and sediment transport observed in native plant communities, especially those dominated by widely spaced shrubs.

Post-process image analysis for the forward-facing camera could employ the same techniques discussed above and, with development time and improvements with real-time image processing speeds, could potentially be used to avoid obstacles and to keep an obstacle such as a vegetation element in a specific portion of the image, thus allowing autonomous circumnavigation of the obstacle. Forward images could also be used as an even earlier indicator than the down-facing camera of a changing surface requiring refinement of robot gait.

(a) D-RHex with forward facing camera

(b) A sample image taken by the forward facing GoPro camera

Figure 9: D-RHex with forward facing camera and sample image

Addressing individual shrubs (or other obstacles) and examining the effects

that they have on metrics of interest during a wind event such as wind direction, strength, and saltation should be possible with our existing system. In principle, we already have the ability to have accurate metric registration of 3DOF instrument pose relative to a shrub. Obstacles of interest such as shrubs are easily visible using LIDAR, as can be seen in Figure 3, and previous research in our group at Penn has addressed a method for accurate registration using the X-RHex platform for active visual servoing [96] using a color camera. Furthermore, active servoing could be used in conjunction with a new sensor discussed in Section 3.2.1 to gather information about the obstacle itself while also collecting data about wind events related to it.

3.2 New sensors under development

Given the wealth of data available through the hardware already discussed, it is possible to derive additional "sensors" without any extra necessary payload. So far we have begun development on two such sensors: One is a classification of obstacles as porous or solid based on a LIDAR reading, and the other is a penetration resistance estimation method using the robot's leg as a soil penetration tool.

3.2.1 Obstacle porosity detection

One of the main assessments human scientists use in aeolian research surveys is of environmental "roughness," a metric which is determined in large part by features of vegetation in the area. In order to determine relevant features of the vegetation in the area, an autonomous robot will need a color camera and depth information. Any sort of depth information obtained from bright-light settings to supplement RGB camera data is invariably obtained by a laser range finder [97] [98], simultaneous analysis of multiple images [99], or through supplementation of multiple image analysis by some other sensor such as a GPS [100]. Fortunately, we already have mounted on D-RHex a Hokuyo laser scanner and a forward-facing camera, and can simply use these sensors for this extra level of analysis.

We have begun development of an obstacle porosity classification system using only a Hokuyo laser scanner [101]. Individual pixels in a scan are classified as coming from an open area, a porous obstacle (such as a bush or a branch), and a solid obstacle (such as a boulder or a tree) by looking at the distribution of depths sensed in a small "window" around the pixel in space and time. This system could be made usable to the aeolian science community by retraining the classifier, which currently detects trees and bushes, on a new dataset classified by our aeolian research science collaborators specific to the desert environments of study. Accuracy could be improved and validation in-field could be made possible by pairing classifications with a forward-facing color camera. Towards this goal, we collected LIDAR scans of obstacles in the Jornada and White Sands dune fields (see Figure 3 for an example LIDAR scan from White Sands).

3.2.2 Penetration resistance

A penetrometer is not currently used in any wind erosion prediction applications. However, it might provide an indication of the surface susceptibility to wind erosion of different soils. This has not been done in the past but this application of D-RHex might help us develop a data set for testing with wind erosion models. The use of a pocket penetrometer for use in aeolian processes has been described by [102]. Physical, chemical, and biological properties of crusts are related to crust strength, which is related to soil erodibility [103]. The D-RHex can be used to rapidly collect data on crust and soil surface strength to assess wind erosion potential. This information is not currently available. Use of the D-RHex to measure soil strength with the soil penetrometer will help develop new models to predict wind erodibility of soils that would be novel and valuable new contributions to model parameterizations.

The penetrometer could also provide important feedback for the robot to assess its own performance and avoid potential known opportunities for failure. Because soil behavior and therefore robot performance will vary greatly with features of the soil, it is vitally important for an autonomous robot to be able to assess features of the soil during operation to avoid getting irretrievably stuck. The packing density of the material is a metric which is of great interest to the roboticists attempting to solve locomotor problems: This parameter is of primary importance to determining the behavior of dry, granular material interacting with small vehicles that rely on a solidification of the material for fast locomotion, because the phase transition from fluid to solid behavior of idealized granular media is a function of depth and packing density [104].

Unfortunately, packing density promises to vary greatly within the environment of study, both as a function of the variability of granule size, shape and makeup and because of the aeolian processes that lead to development of dunes. Sand particle shape has been shown to have large effects on the behavior of the sand at the macroscopic level, including packing density and strain properties of sandy soils. Furthermore, the natural variety of increases in particle-particle friction lead in particular to increases in critical state friction angle and compressibility under zero-lateral strain loading [105]. Meanwhile, packing density in particular has been shown to vary from completely jammed to loose within one ripple on a dune [106]. Different faces of transverse dunes will also likely have different behavior, because they grow from erosion and deposition events [107], causing different faces to have different dominant particle sizes and shapes, which is known to affect the packing density and strain properties of sandy soils, due in part to increases in critical state friction angles [105].

We have been developing a method to measure penetration resistance that relies only on motor current draw required to push a leg to a pre-determined depth below the surface of the sand. We verified that current draw from the motors used in the robot's legs correlates linearly with force by linearizing the motion of the motor with a ball screw and commanding motor positions, taking measurements with a force plate. We also verified that forces produced through rotation of the compliant robot c-leg were linearly correlated with commanded

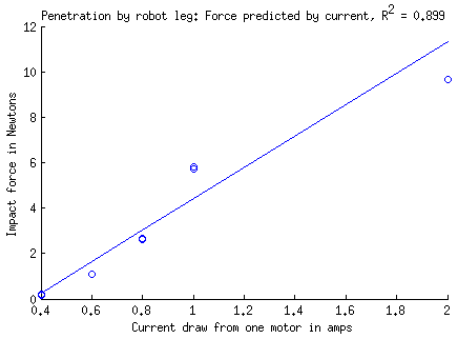

(a) Current draw required for the robot leg achieve a pre-set depth

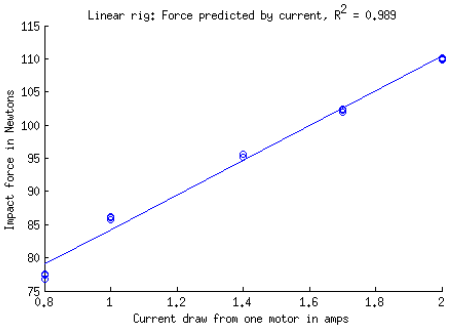

(b) Current draw required for a motor of the same type as in the robot leg to depress a force plate to a pre-set depth, linearized and geared by a ballscrew

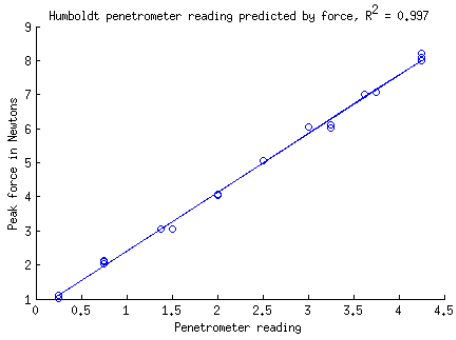

(c) Readings taken with a hand-held Humboldt pocket penetrometer on the same forceplate

(d) Leg penetration at the White Sands national monument

Figure 10: Experimental verification of the robot leg as a penetrometer

motor positions.

4 Mobility challenges in aeolian and dune research-relevant environments

4.1 Dune crest traversals

Dune crest traversals are of interest to aeolean scientists because of the abundance of data that can be collected near the surface of the crest. Saltation occurs primarily in the several inches above the dune crest, but not much is known about how this varies along the crest. Robots provide a great opportunity to rapidly gather these measurements at multiple points along the dune

crest without significantly disturbing the dune. We hand-tuned an alternating tripod gait to minimize sand disturbance during slow traversals. An example robot track is shown in Figure 11b.

The robot was in general able to successfully traverse dune crests. The only failures occurred when the human operator mistakenly steered the robot onto the slip face. One such failure is shown in Figure 11a. Because the robot is typically unable to ascend steep slip faces, it was forced to descend the dune and start the crest traversal again. This problem is exacerbated by the fact that on non-fragile terrains the robot is able to steer quite well but this becomes more difficult on fragile substrates. In future autonomous experiments the main challenge will be sensing the slip face to avoid leaving the crest. This could be accomplished using a LIDAR device to measure the dune curvature in front of the robot. Future work will also concentrate on better modeling of the leg-substrate interaction, possibly using a self-manipulation framework [89]. Using this framework we hope to better take advantage of RHex's steering affordance in granular media.

4.2 Fast traversals

Rapid traversal over a dune crest could prove quite valuable for gathering aeolean science data as in theory it is possible to take measurements at multiple locations using a single platform in a short enough time to approximate the measurements as being taken simultaneously. This would allow a single platform to accomplish what previously would require multiple robots or base stations.

Fast crest traversals were accomplished by first tuning up a fast gait using the Nelder-Meade algorithm to optimize for speed and efficiency. GPS data was used to get the robot's speed during these tests and onboard measurements were taken to estimate the robot's energy expenditure. Once a fast gait was found, it was used on a long dune crest. Two fast traversal runs were then done on a dune with a particularly abrupt slip face drop off as shown in Figure 12. The robot was run as close as possible to the slip face drop off because in a real scenario this is the area where the robot would stop to take measurements. In each instance the robot was able to traverse the crest for a short period of time before an operator error pushed it onto the slip face.

It is apparent that rapid crest traversals are quite challenging for the robot due to the increased risks of leaving the crest for the slip face. Particularly difficult are abrupt drop-offs such as shown in Figure 12 which decrease the steering margin of error. At high speeds even a small steering error can move the robot off of the crest. However even at high speeds a true robot failure such as flipping never occurred: The robot merely traveled down the slip face to the floor of the desert. Rapid robot gaits obviously would be useful in other scenarios such as rapidly traveling from dune to dune across the flat desert floor. However, only dune crests were tested in this initial run as we feel that this poses the most adversarial terrain to the robot.

Another problem with high speed locomotion is that it causes greater disturbance of the substrate than slow speed locomotion due to the larger leg forces.

(a) Dune crest traversal failure. The tracks show the robot's path as it traveled along the dune crest. Near the top of the dune the human operator mistakenly veered the robot onto the slip face and it was unable to ascend directly back to the top.

(b) Close-up of robot tracks with a human footprint in the upper left corner for comparison.

Figure 11: Slow dune crest traversals.

Figure 12: Dune where fast traversals took place.

It is unlikely that gait changes would reduce the disturbance to be less than that of a slow robot gait, however morphological adaptations such as those proposed in Section 5 could mitigate such disturbances. In the case where the robot should not disturb the substrate it would thus be advisable to use a slow gait until morphological improvements have been made.

4.3 Vertical climbs on slip faces of dunes

At White Sands we experimented with vertical climbs on the slip face side of the dune, where inclines frequently exceed 25°. e found this to be a challenging environment for the robot. While D-RHex could potentially climb to any point on a dune, even on the slip face, by climbing up the crest and walking or sliding down to the point of interest, walking vertically up a slip face in excess of 25° or at an angle from the base of the dune up the slip face towards a predetermined location was very challenging.

As a first-pass attempt to improve locomotion, we compared several gaits:

1. Our standard alternating tripod gait, in which the middle leg on the left moves in sync with the front and back legs on the right and the other three legs move in sync one half of a phase off
2. A "slow pronk," in which all six legs recirculated together, which involved a period of time during which the belly of the robot made contact with the ground
3. A crawl gait, in which the six legs moved one at a time in the following order: back left, back right, middle left, middle right, front left, front right. This ensured that five legs were on the ground at any given time
4. A "six-legged bound," in which the back two legs moved together, then the middle two legs moved together, and then the front two legs moved together

We tested each of these gaits on a range of natural inclines from 17 to 28. Conditions for any test with any individual gait were impossible to completely replicate with different gaits since the robot tracks left in the slip face altered the locomotion problem, so we tested different gaits on similar dune faces with similar inclines (within one degree of inclination). We kept our speed at 0.3 m/s, which is far slower than maximum, in order to avoid damaging the dune face.

Results indicated that if one gait could achieve locomotion at a particular incline, all gaits could achieve locomotion, with the exception of the six-legged bound. This gait tended to pitch backwards away from the dune, making the front legs unable to make contact with the dune face, such that the robot was unable to make forward progress. All gaits began failing at $27° \pm 1$. However, the failure modes for the gaits were different. See Figure 13 for further discussion and the supplemental video to this technical report for examples of the different gaits in action.

The alternating tripod failed because the back legs would hit their thermal limit and the motors stalled out. We aborted any test in which the legs stalled in two steps in a row in order to preserve robot health, and on inclines in excess of 27°, the back legs would stall in the first few steps. It is possible that an "alternating bipod" gait, where the first two sets of legs alternate in a trot-like gait and the back legs recirculate together, could provide the stability benefits of the alternating tripod gait while protecting the rear legs.

The slow pronk failed when the robot would successfully take a step up the dune face and slide back down again while recirculating its legs in the air. It could continue in this failure mode indefinitely without motor damage, but also without making progress. If the robot could be prevented from sliding back down the dune, forward progress should in principle be possible. We are exploring the benefits of two possible methods for reducing downward slippage, both based on the same concept: The use of some kind of under-belly horizontal fins to dig into the sand and "catch" the robot before it slides down, or holding the middle legs in position at a depth 1-2 inches below the robot's belly to catch the robot while the other four legs are recirculating.

The crawl gait failed in the same manner as the alternating tripod gait, with the back legs stalling out; again, it is possible that performance could be improved by moving the back legs together and crawling with only the front four legs.

Finally, the six-legged bound failed because of backward pitching. We anticipate that performance could be improved by placing a weight on the front of the robot to encourage forward pitching, which would benefit the robot for any gait since the forces on the back legs are straining to the robot in any gait.

One final failure mode, which was very general and impossible to quantify in the highly variable natural dune environment, was the predisposition of the robots to lose control in the yaw direction. Qualitatively, it was extremely difficult to steer the robot going vertically up a slip face: the steeper the angle of incline, the more likely the robot was to fall slightly to the left or right, and if the robot fell slightly off center, it was difficult to turn it back towards the top of the dune. We are investigating alternative turning methods to improve performance.

5 Potential morphological and behavioral adaptations

Some of the challenge in ascending steep, sandy inclines could be addressed by simple morphological adaptations or minor behavioral adaptations. We plan to explore the efficacy of the following changes in future experiments and desert trips.

1. *Wider legs.* Simply being able to spread the forces from footfall could reduce the probability of a substrate failure.

(a) A successful crawl ascent at 25.75 degrees of incline.

(b) The back left leg has stalled out and the robot is unable to make further progress at 27.05 degrees.

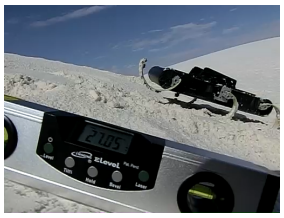

(c) The crawl pitched backwards far enough that the front two legs had difficulty making contact with the ground.

(d) A successful slow pronk at 26.40 degrees.

(e) Here the slow pronk is failing on softer, lighter sand at 24.50 degrees of incline.

(f) The alternating tripod gait failed when rear leg motors stalled.

Figure 13: Still images of failure modes of different gaits

2. *More powerful motors.* Another possibility would be motors with increased power or cooling capacity. One of the main failure conditions was that the rear legs would stall out on steep inclines, particularly when forced to work independently.

3. *Fins.* Adding horizontal strips of stiff material to the underside of the robot body could allow the robot to "grip" the failing substrate and not slide back down, as it did during the slow pronk.

4. *Bigger treads or cleats.* The treads filled with sand immediately and were useless for grip. By increasing the size of the treads, we might prevent their filling up with sand.

5. *Moving the center of mass.* One of the failure modes on steep inclines was that the robot would pitch backwards. By moving the center of mass to the front of the robot, we might be able to discourage this pitching enough to keep the robot from pitching backwards and failing to connect its legs with the substrate.

6. *Using the middle legs for friction.* In addition to or instead of using fins for the slow pronk, it might be beneficial to press the middle legs into the

sand to "hold" the robot in place while the front and back legs recirculate.

6 Conclusions and future work

We conclude based on this trip to the Jornada and White Sands research deserts that the D-RHex in its current form is adequate to be used as a platform for aeolian and desert research, but that dramatic improvements could be conferred by careful attention to the mobility issues discovered at White Sands. We have confirmed that the robot is able to carry a sufficiently large sensor payload to take measurements of interest while locomoting in a desert environment, and the locomotion challenges are not insurmountable. We have already begun work to address several of these challenges, in particular those related to vertical climbs on dune faces with steep angles, and will be testing some improvements in our next desert trip to the Tenggre in Ningxia province, China this fall.

Acknowledgement

This work is supported in part by the International S&T Cooperation Program of China (Ministry of Science and Technology) under grant # 2011DFA11780, in part by the United States National Science Foundation under grant #1028237, and in part by the University of Pennsylvania. We thank the staff of the Jornada Basin Long Term Ecological Research program and David Bustos, Chief of Resource Management White Sands National Monument, for their cooperation in planning and executing these experiments as well as their onsite hospitality throughout our visits.

References

[1] G. Muscato, D. Caltabiano, S. Guccione, D. Longo, M. Coltelli, A. Cristaldi, E. Pecora, V. Sacco, P. Sim, G. Virk, *et al.*, "Robovolc: a robot for volcano exploration result of first test campaign," *Industrial Robot: An International Journal*, vol. 30, no. 3, pp. 231–242, 2003.

[2] J. Porter, P. Arzberger, H.-W. Braun, P. Bryant, S. Gage, T. Hansen, P. Hanson, C.-C. Lin, F.-P. Lin, T. Kratz, *et al.*, "Wireless sensor networks for ecology," *BioScience*, vol. 55, no. 7, pp. 561–572, 2005.

[3] H. McSween, R. Arvidson, J. Bell, D. Blaney, N. Cabrol, P. Christensen, B. Clark, J. Crisp, L. Crumpler, D. Des Marais, *et al.*, "Basaltic rocks analyzed by the spirit rover in gusev crater," *Science*, vol. 305, no. 5685, pp. 842–845, 2004.

[4] R. V. Morris, S. W. Ruff, R. Gellert, D. W. Ming, R. E. Arvidson, B. C. Clark, D. Golden, K. Siebach, G. Klingelhöfer, C. Schröder, *et al.*, "Iden-

tification of carbonate-rich outcrops on mars by the spirit rover," *Science*, vol. 329, no. 5990, pp. 421–424, 2010.

[5] A. Mainwaring, D. Culler, J. Polastre, R. Szewczyk, and J. Anderson, "Wireless sensor networks for habitat monitoring," in *Proceedings of the 1st ACM international workshop on Wireless sensor networks and applications*, pp. 88–97, ACM, 2002.

[6] T. Arampatzis, J. Lygeros, and S. Manesis, "A survey of applications of wireless sensors and wireless sensor networks," in *Intelligent Control, 2005. Proceedings of the 2005 IEEE International Symposium on, Mediterrean Conference on Control and Automation*, pp. 719–724, IEEE, 2005.

[7] P. Tokekar, D. Bhadauria, A. Studenski, and V. Isler, "A robotic system for monitoring carp in minnesota lakes," *Journal of Field Robotics*, vol. 27, no. 6, pp. 779–789, 2010.

[8] N. E. Leonard, D. A. Paley, F. Lekien, R. Sepulchre, D. M. Fratantoni, and R. E. Davis, "Collective motion, sensor networks, and ocean sampling," *Proceedings of the IEEE*, vol. 95, no. 1, pp. 48–74, 2007.

[9] D. Richard Blidberg, R. M. Turner, and S. G. Chappell, "Autonomous underwater vehicles: Current activities and research opportunities," *Robotics and Autonomous Systems*, vol. 7, no. 2, pp. 139–150, 1991.

[10] H. Widditsch, "Spurv-the first decade," tech. rep., DTIC Document, 1973.

[11] W. Nodland, T. Ewart, W. Bendiner, J. Miller, and E. Aagaard, "Spurv ii-an unmanned, free-swimming submersible developed for oceanographic research," in *OCEANS 81*, pp. 92–98, IEEE, 1981.

[12] J. Jalbert, "Eave-east field test results," in *OCEANS 1984*, pp. 582–587, IEEE, 1984.

[13] H. Clark, "New seafloor observatory networks in support of ocean science research," in *OCEANS, 2001. MTS/IEEE Conference and Exhibition*, vol. 1, pp. 245–250, IEEE, 2001.

[14] M. C. Gregg, "The study of mixing in the ocean: A brief history," *Oceanography*, vol. 4, no. 1, pp. 39–45, 1991.

[15] J. Sherman, R. E. Davis, W. Owens, and J. Valdes, "The autonomous underwater glider Spray," *Oceanic Engineering, IEEE Journal of*, vol. 26, no. 4, pp. 437–446, 2001.

[16] C. C. Eriksen, T. J. Osse, R. D. Light, T. Wen, T. W. Lehman, P. L. Sabin, J. W. Ballard, and A. M. Chiodi, "Seaglider: A long-range autonomous underwater vehicle for oceanographic research," *Oceanic Engineering, IEEE Journal of*, vol. 26, no. 4, pp. 424–436, 2001.

[17] O. Schofield, J. Kohut, D. Aragon, L. Creed, J. Graver, C. Haldeman, J. Kerfoot, H. Roarty, C. Jones, D. Webb, *et al.*, "Slocum gliders: Robust and ready," *Journal of Field Robotics*, vol. 24, no. 6, pp. 473–485, 2007.

[18] D. L. Rudnick, R. E. Davis, C. C. Eriksen, D. M. Fratantoni, and M. J. Perry, "Underwater gliders for ocean research," *Marine Technology Society Journal*, vol. 38, no. 2, pp. 73–84, 2004.

[19] J. K. Hart and K. Martinez, "Environmental sensor networks: A revolution in the earth system science?," *Earth-Science Reviews*, vol. 78, no. 3, pp. 177–191, 2006.

[20] M. Caccia, R. Bono, G. Bruzzone, E. Spirandelli, G. Veruggio, A. Stortini, and G. Capodaglio, "Sampling sea surfaces with SESAMO: an autonomous craft for the study of sea-air interactions," *Robotics & Automation Magazine, IEEE*, vol. 12, no. 3, pp. 95–105, 2005.

[21] M. A. Moline, S. M. Blackwell, C. Von Alt, B. Allen, T. Austin, J. Case, N. Forrester, R. Goldsborough, M. Purcell, and R. Stokey, "Remote environmental monitoring units: An autonomous vehicle for characterizing coastal environments," *Journal of Atmospheric and Oceanic Technology*, vol. 22, no. 11, pp. 1797–1808, 2005.

[22] J. D. Lundquist, D. R. Cayan, and M. D. Dettinger, "Meteorology and hydrology in yosemite national park: A sensor network application," in *Information Processing in Sensor Networks*, pp. 518–528, Springer, 2003.

[23] A. Elfes, S. Siqueira Bueno, M. Bergerman, and J. Ramos Jr, "A semi-autonomous robotic airship for environmental monitoring missions," in *Robotics and Automation, 1998. Proceedings. 1998 IEEE International Conference on*, vol. 4, pp. 3449–3455, IEEE, 1998.

[24] L. L. Whitcomb, "Underwater robotics: Out of the research laboratory and into the field," in *Robotics and Automation, 2000. Proceedings. ICRA'00. IEEE International Conference on*, vol. 1, pp. 709–716, IEEE, 2000.

[25] J. Partan, J. Kurose, and B. N. Levine, "A survey of practical issues in underwater networks," *ACM SIGMOBILE Mobile Computing and Communications Review*, vol. 11, no. 4, pp. 23–33, 2007.

[26] D. J. Stilwell and B. E. Bishop, "Platoons of underwater vehicles," *Control Systems, IEEE*, vol. 20, no. 6, pp. 45–52, 2000.

[27] M. Caccia, M. Bibuli, R. Bono, and G. Bruzzone, "Basic navigation, guidance and control of an unmanned surface vehicle," *Autonomous Robots*, vol. 25, no. 4, pp. 349–365, 2008.

[28] J. E. Manley, "Unmanned surface vehicles, 15 years of development," in *OCEANS 2008*, pp. 1–4, IEEE, 2008.

[29] M. Caccia, "Autonomous surface craft: prototypes and basic research issues," in *Control and Automation, 2006. MED'06. 14th Mediterranean Conference on*, pp. 1–6, IEEE, 2006.

[30] J. E. Manley, A. Marsh, W. Cornforth, and C. Wiseman, "Evolution of the autonomous surface craft autocat," in *Oceans 2000 MTS/IEEE Conference and Exhibition*, vol. 1, pp. 403–408, IEEE, 2000.

[31] J. Curcio, J. Leonard, J. Vaganay, A. Patrikalakis, A. Bahr, D. Battle, H. Schmidt, and M. Grund, "Experiments in moving baseline navigation using autonomous surface craft," in *OCEANS, 2005. Proceedings of MTS/IEEE*, pp. 730–735, IEEE, 2005.

[32] D. Smallwood, R. Bachmayer, and L. Whitcomb, "A new remotely operated underwater vehicle for dynamics and control research," in *Proceedings of the 11th International Symposium on Unmanned Untethered Submersible Technology*, pp. 370–377, 1999.

[33] M. A. Batalin and G. S. Sukhatme, "Coverage, exploration and deployment by a mobile robot and communication network," *Telecommunication Systems*, vol. 26, no. 2-4, pp. 181–196, 2004.

[34] M. Trincavelli, M. Reggente, S. Coradeschi, A. Loutfi, H. Ishida, and A. J. Lilienthal, "Towards environmental monitoring with mobile robots," in *Intelligent Robots and Systems, 2008. IROS 2008. IEEE/RSJ International Conference on*, pp. 2210–2215, IEEE, 2008.

[35] M. A. Batalin and G. S. Sukhatme, "Sensor coverage using mobile robots and stationary nodes," in *ITCom 2002: The Convergence of Information Technologies and Communications*, pp. 269–276, International Society for Optics and Photonics, 2002.

[36] R. Szewczyk, E. Osterweil, J. Polastre, M. Hamilton, A. Mainwaring, and D. Estrin, "Habitat monitoring with sensor networks," *Communications of the ACM*, vol. 47, no. 6, pp. 34–40, 2004.

[37] I. J. Walker, "Physical and logistical considerations of using ultrasonic anemometers in aeolian sediment transport research," *Geomorphology*, vol. 68, no. 1, pp. 57–76, 2005.

[38] V. Etyemezian, G. Nikolich, S. Ahonen, M. Pitchford, M. Sweeney, R. Purcell, J. Gillies, and H. Kuhns, "The portable in situ wind erosion laboratory (pi-swerl): A new method to measure pm¡ sub¿ 10¡/sub¿ windblown dust properties and potential for emissions," *Atmospheric Environment*, vol. 41, no. 18, pp. 3789–3796, 2007.

[39] C. H. Hugenholtz, N. Levin, T. E. Barchyn, and M. C. Baddock, "Remote sensing and spatial analysis of aeolian sand dunes: A review and outlook," *Earth-Science Reviews*, vol. 111, no. 3, pp. 319–334, 2012.

[40] S. Engelstaedter, I. Tegen, and R. Washington, "North african dust emissions and transport," *Earth-Science Reviews*, vol. 79, no. 1, pp. 73–100, 2006.

[41] I. Katra and N. Lancaster, "Surface-sediment dynamics in a dust source from spaceborne multispectral thermal infrared data," *Remote sensing of Environment*, vol. 112, no. 7, pp. 3212–3221, 2008.

[42] S. Scheidt, N. Lancaster, and M. Ramsey, "Eolian dynamics and sediment mixing in the gran desierto, mexico, determined from thermal infrared spectroscopy and remote-sensing data," *Geological Society of America Bulletin*, vol. 123, no. 7-8, pp. 1628–1644, 2011.

[43] S. Scheidt, M. Ramsey, and N. Lancaster, "Determining soil moisture and sediment availability at white sands dune field, new mexico, from apparent thermal inertia data," *Journal of Geophysical Research: Earth Surface (2003–2012)*, vol. 115, no. F2, 2010.

[44] P. Vermeesch and N. Drake, "Remotely sensed dune celerity and sand flux measurements of the world's fastest barchans (bodele, chad)," *Geophysical Research Letters*, vol. 35, no. 24, 2008.

[45] C. Bristow, G. Duller, and N. Lancaster, "Age and dynamics of linear dunes in the namib desert," *Geology*, vol. 35, no. 6, pp. 555–558, 2007.

[46] J. M. Nield, J. King, G. F. Wiggs, J. Leyland, R. G. Bryant, R. C. Chiverrell, S. E. Darby, F. D. Eckardt, D. S. Thomas, L. H. Vircavs, *et al.*, "Estimating aerodynamic roughness over complex surface terrain," *Journal of Geophysical Research: Atmospheres*, vol. 118, no. 23, pp. 12–948, 2013.

[47] J. M. Nield, G. F. Wiggs, and R. S. Squirrell, "Aeolian sand strip mobility and protodune development on a drying beach: examining surface moisture and surface roughness patterns measured by terrestrial laser scanning," *Earth Surface Processes and Landforms*, vol. 36, no. 4, pp. 513–522, 2011.

[48] H. J. Moore, D. B. Bickler, J. A. Crisp, H. J. Eisen, J. A. Gensler, A. F. Haldemann, J. R. Matijevic, L. K. Reid, and F. Pavlics, "Soil-like deposits observed by Sojourner, the Pathfinder rover," *Journal of Geophysical Research: Planets (1991–2012)*, vol. 104, no. E4, pp. 8729–8746, 1999.

[49] J. E. Bares and D. S. Wettergreen, "Dante II: Technical description, results, and lessons learned," *The International Journal of Robotics Research*, vol. 18, no. 7, pp. 621–649, 1999.

[50] J. Bares, M. Hebert, T. Kanade, E. Krotkov, T. Mitchell, R. Simmons, and W. Whittaker, "Ambler: An autonomous rover for planetary exploration," *Computer*, vol. 22, no. 6, pp. 18–26, 1989.

[51] R. Volpe, J. Balaram, T. Ohm, and R. Ivlev, "The Rocky 7 Mars rover prototype," in *Intelligent Robots and Systems' 96, IROS 96, Proceedings of the 1996 IEEE/RSJ International Conference on*, vol. 3, pp. 1558–1564, IEEE, 1996.

[52] J. Matson, "Unfree Spirit: NASA's Mars rover appears stuck for good," *Scientific American*, vol. 302, no. 4, pp. 16–16, 2010.

[53] R. R. Murphy, "Human-robot interaction in rescue robotics," *Systems, Man, and Cybernetics, Part C: Applications and Reviews, IEEE Transactions on*, vol. 34, no. 2, pp. 138–153, 2004. Available online.

[54] R. Murphy, J. Casper, M. Micire, and J. Hyams, "Assessment of the NIST standard test bed for urban search and rescue," *NIST SPECIAL PUBLICATION SP*, pp. 260–266, 2001. Available online.

[55] J. Casper and R. R. Murphy, "Human-robot interactions during the robot-assisted urban search and rescue response at the World Trade Center," *Systems, Man, and Cybernetics, Part B: Cybernetics, IEEE Transactions on*, vol. 33, no. 3, pp. 367–385, 2003. Available online.

[56] K. Havstad, W. Kustas, A. Rango, J. Ritchie, and T. Schmugge, "Jornada experimental range: A unique arid land location for experiments to validate satellite systems," *Remote Sensing of Environment*, vol. 74, no. 1, pp. 13–25, 2000.

[57] R. Gibbens, J. Tromble, J. Hennessy, and M. Cardenas, "Soil movement in mesquite dunelands and former grasslands of southern new mexico from 1933 to 1980," *Journal of Range Management*, pp. 145–148, 1983.

[58] D. A. Gillette and A. M. Pitchford, "Sand flux in the northern chihuahuan desert, new mexico, usa, and the influence of mesquite-dominated landscapes," *Journal of Geophysical Research: Earth Surface (2003–2012)*, vol. 109, no. F4, 2004.

[59] J. King, W. Nickling, and J. Gillies, "Aeolian shear stress ratio measurements within mesquite-dominated landscapes of the chihuahuan desert, new mexico, usa," *Geomorphology*, vol. 82, no. 3, pp. 229–244, 2006.

[60] J. A. Gillies, J. M. Nield, and W. G. Nickling, "Wind speed and sediment transport recovery in the lee of a vegetated and denuded nebkha within a nebkha dune field," *Aeolian Research*, vol. 12, pp. 135–141, 2014.

[61] S. Fryberger, "Geological overview of white sands national monument," *A viable from: http://www. nps. gov/whsa*, 2000.

[62] G. Kocurek, M. Carr, R. Ewing, K. G. Havholm, Y. Nagar, and A. Singhvi, "White sands dune field, new mexico: age, dune dynamics and recent accumulations," *Sedimentary Geology*, vol. 197, no. 3, pp. 313–331, 2007.

[63] R. P. Langford, "The holocene history of the white sands dune field and influences on eolian deflation and playa lakes," *Quaternary International*, vol. 104, no. 1, pp. 31–39, 2003.

[64] E. D. McKee, "Structures of dunes at white sands national monument, new mexico (and a comparison with structures of dunes from other selected areas) 1," *Sedimentology*, vol. 7, no. 1, pp. 3–69, 1966.

[65] E. N. Eastwood, G. Kocurek, D. Mohrig, and T. Swanson, "Methodology for reconstructing wind direction, wind speed and duration of wind events from aeolian cross-strata," *Journal of Geophysical Research: Earth Surface (2003–2012)*, vol. 117, no. F3, 2012.

[66] R. C. Ewing and G. A. Kocurek, "Aeolian dune interactions and dune-field pattern formation: White sands dune field, new mexico," *Sedimentology*, vol. 57, no. 5, pp. 1199–1219, 2010.

[67] R. P. Langford, J. M. Rose, and D. E. White, "Groundwater salinity as a control on development of eolian landscape: An example from the white sands of new mexico," *Geomorphology*, vol. 105, no. 1, pp. 39–49, 2009.

[68] D. J. Jerolmack, R. C. Ewing, F. Falcini, R. L. Martin, C. Masteller, C. Phillips, M. D. Reitz, and I. Buynevich, "Internal boundary layer model for the evolution of desert dune fields," *Nature Geoscience*, vol. 5, no. 3, pp. 206–209, 2012.

[69] M. D. Reitz, D. J. Jerolmack, R. C. Ewing, and R. L. Martin, "Barchan-parabolic dune pattern transition from vegetation stability threshold," *Geophysical Research Letters*, vol. 37, no. 19, 2010.

[70] D. J. Jerolmack, M. D. Reitz, and R. L. Martin, "Sorting out abrasion in a gypsum dune field," *Journal of Geophysical Research: Earth Surface (2003–2012)*, vol. 116, no. F2, 2011.

[71] K. C. Galloway, G. C. Haynes, B. D. Ilhan, A. M. Johnson, R. Knopf, G. A. Lynch, B. N. Plotnick, M. White, and D. E. Koditschek, "X-RHex: A highly mobile hexapedal robot for sensorimotor tasks," 2010.

[72] U. Saranli, M. Buehler, and D. E. Koditschek, "Rhex: A simple and highly mobile hexapod robot," *The International Journal of Robotics Research*, vol. 20, no. 7, pp. 616–631, 2001.

[73] A. M. Johnson, M. T. Hale, G. C. Haynes, and D. E. Koditschek, "Autonomous legged hill and stairwell ascent," in *IEEE International Workshop on Safety, Security, & Rescue Robotics, SSRR*, pp. 134–142, November 2011.

[74] T. Zhang, F. Qian, C. Li, P. Masarati, A. M. Hoover, P. Birkmeyer, A. Pullin, R. S. Fearing, and D. I. Goldman, "Ground fluidization promotes rapid running of a lightweight robot," *The International Journal of Robotics Research*, vol. 32, no. 7, pp. 859–869, 2013.

[75] F. Qian, T. Zhang, C. Li, A. M. Hoover, P. Masarati, P. Birkmeyer, A. O. Pullin, R. S. Fearing, and D. Goldman, "Walking and running on yielding and fluidizing ground.," in *Robotics: Science and Systems*, 2012.

[76] C. Li, P. B. Umbanhowar, H. Komsuoglu, and D. I. Goldman, "The effect of limb kinematics on the speed of a legged robot on granular media," *Experimental mechanics*, vol. 50, no. 9, pp. 1383–1393, 2010.

[77] C. Li, A. M. Hoover, P. Birkmeyer, P. B. Umbanhowar, R. S. Fearing, and D. I. Goldman, "Systematic study of the performance of small robots on controlled laboratory substrates," in *Proceedings of SPIE, Orlando, USA*, vol. 7679, p. 76790Z, 2010.

[78] D. Goldman, H. Komsuoglu, and D. Koditschek, "March of the sandbots," *Spectrum, IEEE*, vol. 46, no. 4, pp. 30–35, 2009.

[79] Y. Ding, S. S. Sharpe, A. Masse, and D. I. Goldman, "Mechanics of undulatory swimming in a frictional fluid," *PLoS computational biology*, vol. 8, no. 12, p. e1002810, 2012.

[80] R. D. Maladen, Y. Ding, C. Li, and D. I. Goldman, "Undulatory swimming in sand: Subsurface locomotion of the sandfish lizard," *Science*, vol. 325, no. 5938, pp. 314–318, 2009.

[81] R. D. Maladen, Y. Ding, P. B. Umbanhowar, A. Kamor, and D. I. Goldman, "Biophysically inspired development of a sand-swimming robot," 2011.

[82] R. D. Maladen, Y. Ding, P. B. Umbanhowar, A. Kamor, and D. I. Goldman, "Mechanical models of sandfish locomotion reveal principles of high performance subsurface sand-swimming," *Journal of The Royal Society Interface*, vol. 8, no. 62, pp. 1332–1345, 2011.

[83] N. Mazouchova, N. Gravish, A. Savu, and D. I. Goldman, "Utilization of granular solidification during terrestrial locomotion of hatchling sea turtles," *Biology letters*, vol. 6, no. 3, pp. 398–401, 2010.

[84] N. Mazouchova, P. B. Umbanhowar, and D. I. Goldman, "Flipper-driven terrestrial locomotion of a sea turtle-inspired robot," *Bioinspiration & biomimetics*, vol. 8, no. 2, p. 026007, 2013.

[85] H. Marvi, C. Gong, M. Travers, N. Gravish, J. Mendelson, R. Hatton, H. Choset, D. Hu, and D. Goldman, "Sidewinding as a control template for climbing on sand," *Bulletin of the American Physical Society*, 2014.

[86] A. G. Winter, *Biologically inspired mechanisms for burrowing in undersea substrates*. PhD thesis, Massachusetts Institute of Technology, 2011.

[87] G. C. Haynes, J. Pusey, R. Knopf, A. M. Johnson, and D. E. Koditschek, "Laboratory on legs: An architecture for adjustable morphology with legged robots," in *Unmanned Systems Technology XIV* (R. E. Karlsen, D. W. Gage, C. M. Shoemaker, and G. R. Gerhart, eds.), vol. 8387, p. 83870W, SPIE, 2012.

[88] A. M. Johnson and D. E. Koditschek, "Robot parkour: The ground reaction complex and dynamic transitions," in *Dynamic Walking*, June 2013.

[89] A. M. Johnson and D. E. Koditschek, "Legged self-manipulation," *IEEE Access*, vol. 1, pp. 310–334, May 2013.

[90] C. Li, T. Zhang, and D. I. Goldman, "A terradynamics of legged locomotion on granular media," *science*, vol. 339, no. 6126, pp. 1408–1412, 2013.

[91] C. H. Hugenholtz and T. E. Barchyn, "Laboratory and field performance of a laser particle counter for measuring aeolian sand transport," *Journal of Geophysical Research: Earth Surface (2003–2012)*, vol. 116, no. F1, 2011.

[92] E. A. Tsvetsinskaya, C. Schaaf, F. Gao, A. Strahler, R. Dickinson, X. Zeng, and W. Lucht, "Relating modis-derived surface albedo to soils and rock types over northern africa and the arabian peninsula," *Geophysical Research Letters*, vol. 29, no. 9, pp. 67–1, 2002.

[93] A. Chappell, S. Van Pelt, T. Zobeck, and Z. Dong, "Estimating aerodynamic resistance of rough surfaces using angular reflectance," *Remote Sensing of Environment*, vol. 114, no. 7, pp. 1462–1470, 2010.

[94] P. Arbelaez, M. Maire, C. Fowlkes, and J. Malik, "Contour detection and hierarchical image segmentation," *Pattern Analysis and Machine Intelligence, IEEE Transactions on*, vol. 33, no. 5, pp. 898–916, 2011.

[95] W. Casaca, A. Paiva, E. Gomez-Nieto, P. Joia, and L. G. Nonato, "Spectral image segmentation using image decomposition and inner product-based metric," *Journal of mathematical imaging and vision*, vol. 45, no. 3, pp. 227–238, 2013.

[96] A. De, K. S. Bayer, and D. E. Koditschek, "Active sensing for dynamic, non-holonomic, robust visual servoing," in *IEEE International Conference on Robotics and Automation*, May 2014.

[97] R. Manduchi, A. Castano, A. Talukder, and L. Matthies, "Obstacle detection and terrain classification for autonomous off-road navigation," *Autonomous robots*, vol. 18, no. 1, pp. 81–102, 2005. Available online.

[98] C. Wellington and A. Stentz, "Online adaptive rough-terrain navigation vegetation," in *Robotics and Automation, 2004. Proceedings. ICRA'04. 2004 IEEE International Conference on*, vol. 1, pp. 96–101, IEEE, 2004. Available online.

[99] M. Pollefeys, D. Nistér, J.-M. Frahm, A. Akbarzadeh, P. Mordohai, B. Clipp, C. Engels, D. Gallup, S.-J. Kim, P. Merrell, *et al.*, "Detailed real-time urban 3D reconstruction from video," *International Journal of Computer Vision*, vol. 78, no. 2-3, pp. 143–167, 2008.

[100] G. Flores, S. Zhou, R. Lozano, and P. Castillo, "A vision and GPS-based real-time trajectory planning for a MAV in unknown and low-sunlight environments," *Journal of Intelligent & Robotic Systems*, pp. 1–9, 2014.

[101] S. Roberts, "Towards a method for obstacle porosity classification."

[102] T. M. Zobeck, G. Sterk, R. Funk, J. L. Rajot, J. E. Stout, and R. S. Van Pelt, "Measurement and data analysis methods for field-scale wind erosion studies and model validation," *Earth Surface Processes and Landforms*, vol. 28, no. 11, pp. 1163–1188, 2003.

[103] N. P. Webb and C. L. Strong, "Soil erodibility dynamics and its representation for wind erosion and dust emission models," *Aeolian Research*, vol. 3, no. 2, pp. 165–179, 2011.

[104] M. Schröter, S. Nägle, C. Radin, and H. L. Swinney, "Phase transition in a static granular system," *EPL (Europhysics Letters)*, vol. 78, no. 4, p. 44004, 2007.

[105] G.-C. Cho, J. Dodds, and J. C. Santamarina, "Particle shape effects on packing density, stiffness, and strength: natural and crushed sands," *Journal of Geotechnical and Geoenvironmental Engineering*, vol. 132, no. 5, pp. 591–602, 2006.

[106] M. Y. Louge, A. Valance, A. Ould el Moctar, and P. Dupont, "Packing variations on a ripple of nearly monodisperse dry sand," *Journal of Geophysical Research: Earth Surface (2003–2012)*, vol. 115, no. F2, 2010.

[107] H. Tsoar, D. G. Blumberg, and Y. Stoler, "Elongation and migration of sand dunes," *Geomorphology*, vol. 57, no. 3, pp. 293–302, 2004.